ELSEVIER

Polymer 42 (2001) 359–373

polymer

www.elsevier.nl/locate/polymer

# Soluble sulfonated naphthalenic polyimides as materials for proton exchange membranes

C. Genies[a], R. Mercier[a,*], B. Sillion[a], N. Cornet[b], G. Gebel[b], M. Pineri[c]

[a]*Laboratoire des Matériaux Organiques à Propriètès Spécifiques, UMR 5041, CNRS, BP 24, 69 390 Vernaison, France*
[b]*CEA/Département de Recherche Fondamentale sur la Matière Condensée, SI3M-Groupe Polymères Conducteurs Ioniques, 17 rue des Martyrs, 38 054 Grenoble cedex 9, France*
[c]*CEA/Département d'Etudes des Matériaux, SPCM, 17 rue des Martyrs, 38 054 Grenoble cedex 9, France*

Received 16 April 2000; accepted 17 May 2000

**Abstract**

Series of sequenced sulfonated naphthalenic polyimides with improved solubility were prepared by polycondensation in *m*-cresol using aromatic diamines containing phenylether bonds and/or bulky groups. Sulfonated polyimides were characterized by NMR and IR spectroscopies. Membranes were prepared by solution casting method and characterized by determining the ion-exchange capacity, water swelling, proton conductivity whereas the morphology of polymer membranes was studied by small angle neutron scattering. 

*Keywords*: Sulfonated polyimides; Polycondensation; Ion-exchange membranes

## 1. Introduction

For many years sulfonated polymers are investigated intensively because of their current and potential applications in many areas [1]. One of the most important applications is their use as an ion selective separator in electrolysis or electrodialysis systems [1]. Many studies were also concerned with water-selective pervaporation membranes containing sulfonated polymers for separation of aqueous organic mixtures [2]. The reverse osmosis as well as gas permeation properties of sulfonated polymers such as sulfonated poly(phenylene oxide) [3–5] or sulfonated polysulfone [6] were also studied. Some work was concerned with the preparation of rigid-rod molecular composites via ionic interactions between a polyelectrolyte host and a reinforcing rigid-rod polymer [7,8]. The compatibilizing effect of such polymers was also mentioned to lead to a real miscibility improved of insoluble polymers [9,10]. These sulfonated polymers have been also used as dopant for water-soluble polyaniline [11]. One more recent and promising application is the ion-conductive membranes for batteries [12] or fuel cells [13–15]. For instance, perfluorosulfonated ionomer (Nafion) membranes have been used for this purpose due to their efficient proton conduction ($10^{-1}$ S cm$^{-1}$ in the fully hydrated protonic form) and long life time [16]. However, the high cost of this ionomer is a major drawback for the development of this technology. Then, lower cost polymers with similar properties are strongly desired as alternative materials. Sulfonated polymers are usually prepared either by sulfonation of a polymer in solution or by post-modification of a polymer film. The originality of our approach for preparing an alternative material is the introduction of ionic groups onto the polyimide backbone [17,18], using a sulfonated monomer. This approach allows us to control both sulfonation degree and ionic group distribution. The first sulfonated polyimides (SPIs) were based on 4,4′-diamino-biphenyl 2,2′-disulphonic acid (BDSA), 4,4′-oxydianiline (ODA) and oxy-diphthalic dianhydride (ODPA) which are commercially available. These polymers called phthalic polyimides were soluble in *m*-cresol but were not enough stable in fuel cell conditions [18]. As second generation sulfonated polyimides based on 1,4,5,8-naphthalene tetracarboxylic dianhydride (NTDA) instead of ODPA were investigated. Swelling measurements, ionic conductivity and fuel cell experiments were performed on these membranes [18] showing that naphthalenic SPIs are promising materials for PEMFC. Unfortunately, their solubility was greatly reduced compared to phthalic SPIs since they are soluble in chlorophenol.

The purpose of this work was to prepare SPIs with an

* Corresponding author. Tel.: +33-04-78-02-22-72; fax: +33-04-78-02-77-38.
*E-mail address:* regis.mercier@lmops.univ.fr (R. Mercier).

0032-3861/01/$ - see front matter 
PII: S0032-3861(00)00384-0

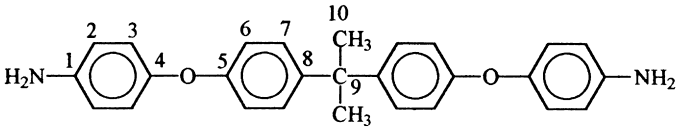

Bis[4-(aminophenoxy)4-phenyl]isopropylidene (pAPI)

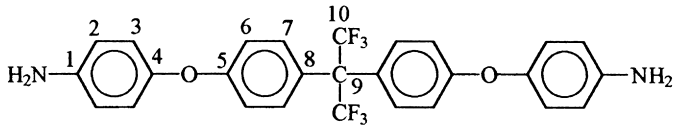

Bis[4-(aminophenoxy)4-phenyl]hexafluoroisopropylidene (pAPFI)

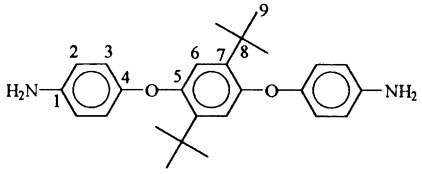

1,4-Bis-(4'-aminophenoxy)-2,5-tertiobutylbenzene (ADTB)

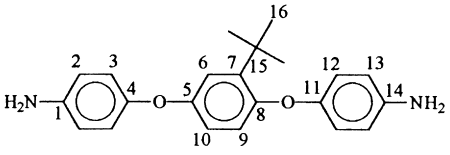

1,4-Bis-(4'-aminophenoxy)-2-tertiobutylbenzene (ATB)

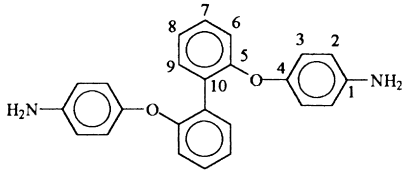

2,2'-(4'-aminophenoxy)biphenyle (ABP)

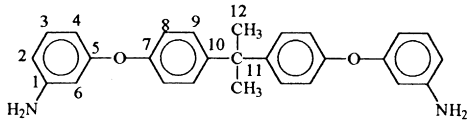

Bis [3-(aminophenoxy)-4-phenyl]isopropylidene (mAPI)

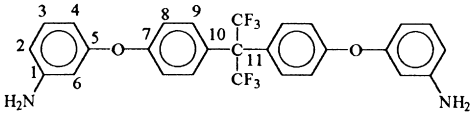

Bis [3-(aminophenoxy)-4-phenyl]hexafluoroisopropylidene (mAPFI)

Fig. 1. Chemical structures of synthesized aromatic diamines.

improved solubility by introducing ether linkages into the main chain or bulky groups as substituent. In this paper, we describe the synthesis and related properties of new naphthalenic copolyimides obtained from BDSA and aryl ether diamines. The preparation of SPIs series with different ion-exchange capacities and sulfonated polyimide block length was also considered which allows us to study structure–properties relationships in terms of water swelling and proton conductivity.

## 2. Experimental part

### 2.1. Starting materials

4-Chloronitrobenzene, 1,3-dinitrobenzene, bisphenol compounds which were used for the synthesis of the different diamines were purchased from commercial source and used as received. Anhydrous potassium carbonate, hydrazine monohydrate, 10% palladium on activated carbon, benzoic acid, triethylamine as well as *N*,*N*-dimethylacetamide (DMAc), *N*,*N*-dimethylformamide (DMF) and *m*-cresol were purchased and used as received. The 4,4′-diamino-biphenyl 2,2′-disulphonic acid (BDSA) obtained from commercial source was purified before polycondensation reaction. The 1,4,5,8-naphthalene tetracarboxylic dianhydride (NTDA) is a commercial product which was dried at 160°C under vacuum before use.

### 2.2. Monomer synthesis

Structures of synthesized diamines are shown in Fig. 1.

#### 2.2.1. bis[4-(Aminophenoxy)4-phenyl]isopropylidene (pAPI)

A 0.5-l three-necked round bottom flash containing 20.0 g ($8.8 \times 10^{-2}$ mol) of bisphenol A, 27.6 g ($1.7 \times 10^{-1}$ mol) of 4-chloronitrobenzene, 48.4 g ($3.5 \times 10^{-1}$ mol) of potassium carbonate and 60 ml of *N*,*N*′-dimethylacetamide (DMAc) were fitted with a magnetic stirrer, condenser, nitrogen pad and thermometer. This mixture was heated to 140°C for 5 h under nitrogen atmosphere. The solution was then cooled down and the insoluble inorganic residue was filtered off. The DMAc was evaporated off. The isolated yellow powder was then washed with methanol and dried at 60°C under vacuum. The crude product was crystallized from isopropanol to obtain 40.7 g of bis[4-(nitrophenoxy)4-phenyl]isopropylidene with a yield of 98.7%. A mixture of 10.0 g ($2.1 \times 10^{-2}$ mol) of dinitro compound, 0.15 g of Pd/C catalyst and 100 ml of ethyl acetate was placed in a hydrogen pressure steel autoclave. When the hydrogen pressure was stabilized, the reaction mixture was filtered to separate the catalyst. After evaporation of the solvent, 8.5 g of the pAPI diamine was obtained, m.p. = 127°C.

$^1$H NMR (d6-DMSO): 1.69 (s, 6H, $H_{10}$); 7.10 (m, 8H, $H_{3,2}$); 7.35 (d, J = 8.9Hz, 4H, $H_6$); 8.22 (d, $J = 8.9$ Hz, 4H, $H_7$).

$^{13}$C NMR (DMSO-d6): 31.12 (2C, $C_{10}$); 41.55 (1C, $C_9$); 115.08 (4C, $C_3$); 116.10 (4C, $C_2$); 121.02 (4C, C6); 127.95 (4C, $C_7$); 143.90 (2C, $C_1$); 145.55 (2C, $C_4$); 145.97 (2C, $C_8$); 156.89 (2C, $C_5$).

#### 2.2.2. bis[4-(Aminophenoxy)4-phenyl] hexafluoroisopropylidene (pAPFI)

The synthesis of bis[4-(nitrophenoxy)4-phenyl]hexafluoroisopropylidene was carried out in the same way as that for bis[4-(nitrophenoxy)4-phenyl]isopropylidene using proper amount of bisphenol 6F, 4-chloronitrobenzene and potassium carbonate. Yield (95.8%). A mixture of 10.0 g ($1.7 \times 10^{-2}$ mol) of obtained dinitro compound, 0.1 g of Pd/C catalyst and 100 ml of ethylacetate was placed in a hydrogen pressure steel autoclave. After stabilization of pressure hydrogen, the reaction mixture was filtered off to separate the catalyst. After evaporation of the solvent, one obtained a brown oily residue which was dissolved in hot ethanol and poured in warm water/ethanol (50/50) mixture with stirring. On cooling, the diamine was crystallized. The precipitated yellow powder was collected by filtration and was dried under vacuum at 60°C. 6.7 g of pAPFI diamine (m.p. = 162°C) was obtained. The yield was 74.4%.

$^1$H NMR (DMSO-d6): 5.05 (sl, 4H, $H_{diamine}$); 6.61 (d, $J =$ 8.6 Hz, 4H, $C_2$); 6.82 (d, $J = 8.6$ Hz, 4H, $C_3$); 6.92 (d, $J = 8.6$ Hz,4H, $C_6$); 7.25 (d, $J = 8.6$ Hz, 4H, $C_7$).

$^{13}$C NMR (DMSO-d6): 63.00 (1C, C9); 115.07 (4C, $C_3$); 116.04 (4C, $C_2$); 121.55 (4C, $C_6$); 125.23 (2C, $C_8$); 131.36 (4C, $C_7$); 144.52 (2C, $C_1$); 146.24 (2C, $C_4$); 159.82 (2C, $C_5$).

#### 2.2.3. 1,4-bis-(4-Aminophenoxy)-2,5-tertiobutylbenzene (ADTB)

The synthesis of 1,4-bis-(4′-nitrophenoxy)-2,5-tertiobutylbenzene was carried out in the same way as that for bis[4-(nitrophenoxy)4-phenyl]isopropylidene using 2,5-tertiobutylhydroquinone, 4-chloronitrobenzene and potassium carbonate. Yield 73.8%. 10.0 g ($2.1 \times 10^{-2}$ mol), of the obtained dinitro compound a tip of spatula of Pd/C and 40 ml ethanol were introduced into a three-necked flask fitted with a magnetic stirrer, condenser, nitrogen pad and a thermometer. This mixture was heated at ethanol reflux temperature. 4.3 g ($8.4 \times 10^{-2}$ mol) of hydrazine, in solution in 20 ml of ethanol, were added dropwise. After the complete addition, the reaction was hold at reflux temperature for 4 h. The hot mixture was then filtered off to remove Pd/C catalyst. Ethanol solvent was evaporated. The obtained residue was washed overnight with petroleum ether. The precipitated brown powder was filtered, dried at 80°C under vacuum. The yield of ADTB diamine (m.p. = 247°C) was 7.8 g (85.8%).

$^1$H NMR (DMSO-d6): 1.23 (s, 18H, $H_9$); 4.87 (sl, 4H, $H_{diamine}$); 6.57 (d, $J = 8.9$ Hz, 4H, $H_2$); 6.64 (s, 2H, $H_6$); 6.69 (d, $J = 8.9$ Hz, 4H, $H_3$).

$^{13}$C NMR (DMSO-d6): 29.62 (6C, $C_9$); 34.92 (2C, $C_8$);

115.00 (4C, $C_2$); 116.95 (2C, $C_6$); 119.30 (4C, $C_3$); 137.50 (2C, $C_7$); 144.29 (2C, $C_1$); 147.10 (2C, $C_4$); 150.67 (2C, $C_5$).

### 2.2.4. 1,4-bis-(4′-Aminophenoxy)-2-tertiobutylbenzene (ATB)

In 0.5-l three-necked flask fitted with a magnetic stirrer, condenser, nitrogen pad and a thermometer, 11.6 g ($7.0 \times 10^{-2}$ mol) of *tert*-butylhydroquinone, 22.0 g ($1.4 \times 10^{-1}$ mol) of 4-chloronitrobenzene, 38.5 g ($2.6 \times 10^{-1}$ mol) of potassium carbonate and 120 ml of DMAc were introduced. The solution were heated at 160°C for 8 h. The reaction mixture was then cooled and filtered off to separate the insoluble inorganic residue. The filtrate was concentrated by evaporation of DMAc and precipitated in methanol. The product was isolated by filtration, washed in methanol and dried under vacuum at 80°C. The yield of 1,4-bis-(4′-nitrophenoxy)-2-tertiobutylbenzene was 25.0 g (96.1%). The hydrogenation of obtained dinitro compound was carried out in the same way as previously. Yield 93.7%, m.p. (DSC) 127°C.

$^1$H NMR (DMSO-d6): 1.34 (s, 9H, $C_{16}$); 4.90 (sl, 4H, $H_{diamine}$); 6.70 (m, 10H, $C_{2,3,12,139,10}$); 6.88 (s, 1H, $C_6$).

$^{13}$C NMR (DMSO-d6): 29.84 (3C, $C_{16}$); 34.56 (1C, $C_{15}$); 114.84 (1C, $C_6$); 115.20 (2C, $C_{13}$); 115.31 (2C, $C_3$); 115.95 (1C, $C_{10}$); 119.57 (1C, $C_9$); 119.64 (2C, $C_{12}$); 120.53 (2C, $C_2$); 140.82 (1C, $C_7$); 144.49 (1C, $C_{11}$); 145.05 (1C, $C_4$); 146.74 (1C, $C_{14}$); 147.89 (1C, $C_1$); 151.75 (1C, $C_8$); 153.47 (1C, $C_5$).

### 2.2.5. 2,2′-(4-Aminophenoxy)biphenyl (ABP)

20.0 g ($1.1 \times 10^{-1}$ mol) of 2,2′-dihydroxybiphenyl, 59.3 g ($4.3 \times 10^{-1}$ mol) of carbonate potassium and 60 ml DMAc were introduced in a three-necked flask fitted with a magnetic stirrer, condenser, nitrogen pad and a thermometer. The mixture was heated at 160°C. 33.9 g ($2.2 \times 10^{-1}$ mol) of 4-chloronitrobenzene in solution in 40 ml of DMAc were added dropwise. The mixture was hold at 160°C for 16 h. After cooling, reaction mixture was filtered off to eliminate insoluble inorganic residue and then the filtrate was precipitated in methanol. The precipitated yellow powder was filtered, washed with water and dried under vacuum at 100°C. The yield of 2,2′-(4′-nitrophenoxy)biphenyl was 31.0 g (78.7%). 10.0 g ($2.3 \times 10^{-2}$ mol) of dinitro compound, a tip of spatula of Pd/C catalyst and 150 ml of ethyl acetate were introduced in a pressure hydrogen steel autoclave. After stabilization of hydrogen pressure, the reaction mixture was filtered off to eliminate the catalyst. Ethyl acetate was evaporated under vacuum. The obtained yellow powder was dried under vacuum at 80°C. The weight of ABP diamine (m.p. = 99°C and 157°C) was 7.3 g and the yield was 73.1%.

$^1$H NMR (DMSO-d6): 4.90 (sl, 4H, $H_{diamine}$); 6.52 (d, $J$ = 8.6 Hz, 4H, $H_2$); 6.66 (m, 6H, $C_{3,6}$); 7.05 (dd, $J$ = 8.0 Hz, 2H, $H_8$); 7.24 (dd, $J$ = 8.0 Hz, 2H, $H_7$); 7.32 (d, $J$ = 4.4 Hz, 2H, $H_9$).

$^{13}$C NMR (DMSO-d6): 115.44 (4C, $C_2$); 116.12 (2C, $C_6$); 121.05 (4C, $C_3$); 121.88 (2C, $C_8$); 128.54 (2C, $C_9$[1]); 129.05 (2C, $C_7$[1]); 131.95 (2C, $C_{10}$); 145.23 (2C, $C_1$); 146.62 (2C, $C_4$); 156.84 (2C, $C_5$).

### 2.2.6. bis[3-(Aminophenoxy)-4-phenyl]isopropylidene (mAPI)

20.0 g ($8.8 \times 10^{-2}$ mol) of bisphenol A, 29.5 g ($1.7 \times 10^{-1}$ mol) of 1,3-dinitrobenzene, 48.4 g ($3.5 \times 10^{-1}$ mol) of carbonate potassium and 100 ml of DMF with 10 ml of toluene were introduced in a three-necked flask fitted with a magnetic stirrer, condenser with a Dean-Stark trap, nitrogen pad and a thermometer. The reaction mixture was heated at 140°C for 17 h. After cooling at room temperature, the mixture was filtered off to eliminate the insoluble inorganic residue. The DMF solvent was evaporated using a rotary evaporator. The precipitated powder was washed with methanol. The dinitro compound was filtered off and dried at 60°C. The yield of bis[3-(nitrophenoxy)-4-phenyl]isopropylidene was 28.1 g (68.1%). 12.0 g ($3.2 \times 10^{-2}$ mol) of this dinitro compound, a tip of spatula of Pd/C catalyst and 80 ml of ethanol were introduced in a three-necked flask fitted with a magnetic stirrer, condenser, nitrogen pad and a thermometer. This mixture was heated at ethanol reflux temperature. Then, 3.2 g ($6.4 \times 10^{-2}$ mol) of hydrazine in solution of 20 ml of ethanol were added dropwise. This reaction mixture was heated at 80°C for 4 h with stirring. After cooling at room temperature, the solution was filtered off to remove the catalyst. The ethanol was then evaporated under vacuum. The isolated powder was washed overnight with petroleum ether filtrated off and dried under vacuum at 60°C. The yield of mAPI diamine (m.p. = 100°C) was 9.9 g (94.4%).

$^1$H NMR (DMSO-d6): 1.62 (s, 6H, $H_{12}$); 5.21 (sl, 4H, $H_{diamine}$); 6.11 (d, $J$ = 9.0 Hz, 2H, $H_2$); 6.18 (s, 2H, $H_6$); 6.31 (d, $J$ = 9.0 Hz, 2H, $H_4$); 6.89 (d, $J$ = 8.6 Hz, 4H, $H_8$); 6.97 (dd, $J$ = 9.0 Hz, 2H, $H_3$); 7.20 (d, $J$ = 8.6 Hz, 4H, $H_9$).

$^{13}$C NMR (DMSO-d6): 30.81 (2C, $C_{12}$); 41.72 (1C, $C_{11}$); 103.89 (2C, $C_6$); 105.98 (2C, $C_4$); 109.39 (2C, $C_2$); 118.16 (4C, $C_8$); 127.96 (4C, $C_9$); 130.16 (2C, $C_3$); 144.99 (2C, $C_{10}$); 150.61 (2C, $C_1$); 154.83 (2C, $C_7$); 157.82 (2C, $C_5$).

### 2.2.7. bis[3-(Aminophenoxy)-4-phenyl] hexafluoroisopropylidene (mAPFI)

The synthesis of bis[3-(nitrophenoxy)-4-phenyl]hexafluoroisopropylidene was carried out in the same way as the for bis[3-(nitrophenoxy)-4-phenyl]isopropylidene using 33.0 g ($8.9 \times 10^{-2}$ mol) of bisphenol 6F and the proper amount of 1,3-dinitrobenzene, (30.0 g, $1.8 \times 10^{-1}$ mol in excess of 10%). The reaction mixture was heated at 160°C for 8 h. After cooling at room temperature, the mixture was filtered off to eliminate the insoluble inorganic residue. The filtrate was concentrated using a rotary evaporator. The precipitated powder obtained was dissolved

[1] Attributions could be reversed.

with dichloromethane, dried and percolated on alumina. Dichloromethane was removed using a rotary evaporator. The obtained compound was dried under vacuum at 80°C. The yield of was 27.9 (26.9%). The hydrogenation of obtained dinitro compound was carried out in the same way as previously. Yield 69.0% (m.p. 127°C).

$^1$H NMR (DMSO-d6): 5.31 (sl, 4H, $H_{diamine}$); 6.21 (d, $J$ = 9.8 Hz, 2H, $H_2$); 6.29 (s, 2H, $H_6$); 6.41 (d, $J$ = 9.8 Hz, 2H, $H_4$); 7.04 (m, 6H, $H_{3,8}$); 7.33 (d, $J$ = 8.6 Hz, 4H, $H_9$).

$^{13}$C NMR (DMSO-d6): 63.30 (1C, $C_{11}$); 104.85 (2C, C6); 106.76 (2C, $C_4$); 110.39 (2C, $C_2$); 117.64 (4C, $C_8$); 126.13 (2C, $C_{10}$), 130.44 (4C, $C_9$); 131.48 (2C, $C_3$); 150,88 (2C, $C_1$); 156.35 (2C, $C_7$); 158.24 (2C, $C_5$).

### 2.3. Polymer synthesis

#### 2.3.1. Sequenced copolyimide preparation

All sequenced polyimides were prepared by analogous procedure. For example, we describe here after a typical procedure for preparation of BDSA/NTDA/mAPI ($r_1 = n_{NTDA}/n_{BDSA} = 4/5$ and $r_2 = n_{BDSA}/n_{mAPI} = 30/70$) sequenced polyimide.

In a three-necked flask fitted with mechanical stirrer, nitrogen pad, 0.3464 g ($10^{-3}$ mol) of BDSA and 0.25 g ($2.4 \times 10^{-3}$ mol) of triethylamine were introduced with 3 g of *m*-cresol. This mixture was stirred until complete dissolution of BDSA. Then 0.2145 g ($8 \times 10^{-4}$ mol) of NTDA and 0.14 g ($1.12 \times 10^{-3}$ mol) of benzoic acid were added. This reaction mixture was then heated at 80°C for 4 h and at 180°C for 14 h. After cooling at room temperature, 0.9579 g ($2.3 \times 10^{-3}$ mol) of mAPI, 0.6794 g ($2.533 \times 10^{-3}$ mol) of NTDA and 0.44 g ($3.54 \times 10^{-3}$ mol) of benzoic acid were added with 6 g of *m*-cresol. The reaction mixture was stirred few minutes at room temperature and then heated at 80°C for 4 h and 180°C for 20 h. Before cooling, 16 g of *m*-cresol were added and the viscous polymer solution was poured into ethyl acetate. The precipitated polyimide was collected by filtration, washed with ethyl acetate and dried under vacuum at 100°C.

#### 2.3.2. Statistic copolyimide preparation

All statistic polyimides were prepared by the same method and we describe only the synthesis procedure of BDSA/NTDA/mAPI ($r_2 = n_{BDSA}/n_{mAPI} = 30/70$).

In a three-necked flask fitted with mechanical stirrer, nitrogen pad, 0.3464 g ($10^{-3}$ mol) of BDSA containing 0.6% water, (determined by thermogravimetric analysis), and 0.25 g ($2.4 \times 10^{-3}$ mol) of triethylamine were introduced with 9 g of *m*-cresol. This mixture was stirred until solubilization of BDSA. Then 0.8939 g ($3.33 \times 10^{-3}$ mol) of NTDA, 0.9578 g ($2.33 \times 10^{-3}$ mol) of mAPI diamine, 0.57 g ($4.66 \times 10^{-3}$ mol) of benzoic acid were added. This reaction mixture was stirred few minutes and then heated at 80°C for 4 h and at 180°C for 20 h.

Before cooling, 3.5 g of *m*-cresol were added and the viscous polymer solution was poured into ethyl acetate. The precipitated polyimide was collected by filtration, washed with ethyl acetate and dried under vacuum at 100°C.

#### 2.3.3. Film preparation

Membranes of naphthalenic sulfonated polyimides were obtained by solution casting at 120°C from the polymer solution in *m*-cresol. The films were dried on hot plate for 2 h at 50°C, 2 h at 100°C and finally 1 h at 150°C. The polymer film was unstuck from the glass plate support by immersion in methanol. Series of tough sulfonated polyimide films were obtained with controlled thickness from 25 to 40 μm.(Membranes were acidified with 0.1 M HCl solution overnight and then rinsed with water. Finally, they were dried overnight at 80°C under vacuum.

### 2.4. Polymer characterization

Both $^1$H and $^{13}$C NMR analysis were performed at 30°C for the monomers and at 80°C for the polymers on a NMR spectrometer (AC250 Brucker). The sulfonated naphthalenic polyimides were dissolved in DMSO-d6. IR spectra were recorded in the 4000–400 cm$^{-1}$ range for the polymers (Nicolet 20 SX). The inherent viscosity values of all polyimides were measured at 0.5 g dl$^{-1}$ in *m*-cresol using an Ubbelohde viscosimeter with the capillary diameter of 0.78 mm. The ionic-exchange capacity (IEC) was measured by classical titration. The membranes were soaked in a saturated NaCl solution. Released protons were titrated using NaOH solution. The IEC values were also confirmed by thermogravimetric analysis. Thermogravimetric data were obtained both on a TG209 NETZSCH under nitrogen at a heating rate of 5°C min$^{-1}$ and on a Setaram TGA92 in flowing nitrogen at a heating rate of 1°C min$^{-1}$. The ionic conductivity of membranes was determined by impedance spectroscopy using a mercury electrode cell. The swelling in water was determined by measuring the uptake of water at room temperature using the weight difference of the swollen to the dry membrane, relative to the dry weight. The membrane was first dried overnight in a vacuum oven at 110°C and weighted. Sample was then immersed in liquid water at room temperature. After several hours of equilibration, the membrane was then wiped dry and quickly weighted. The water uptake WS of membranes is represented as the amount of water per gram of the dry membrane and was determined using the following relation:

$$\mathrm{WS} = \frac{(W_s - W_d)}{W_d} \cdot 100 \text{ (expressed in\%)}$$

where $W_d$ and $W_s$ are the weight of the dry and wet membranes, respectively.

The SANS experiments were performed at the Laboratoire Léon Brillouin (CEA/CNRS, Orphée reactor, Saclay, France) on the PAXE spectrometer. The overall angular range $(5 \times 10^{-3} < q \ (\text{Å}^{-1}) < 0.3$ with $q = 4\pi \sin\theta/\lambda$ where $\theta$ is the scattering angle) was accessed varying the wavelength from $\lambda = 5$ Å to $\lambda = 12$ Å and with a sample

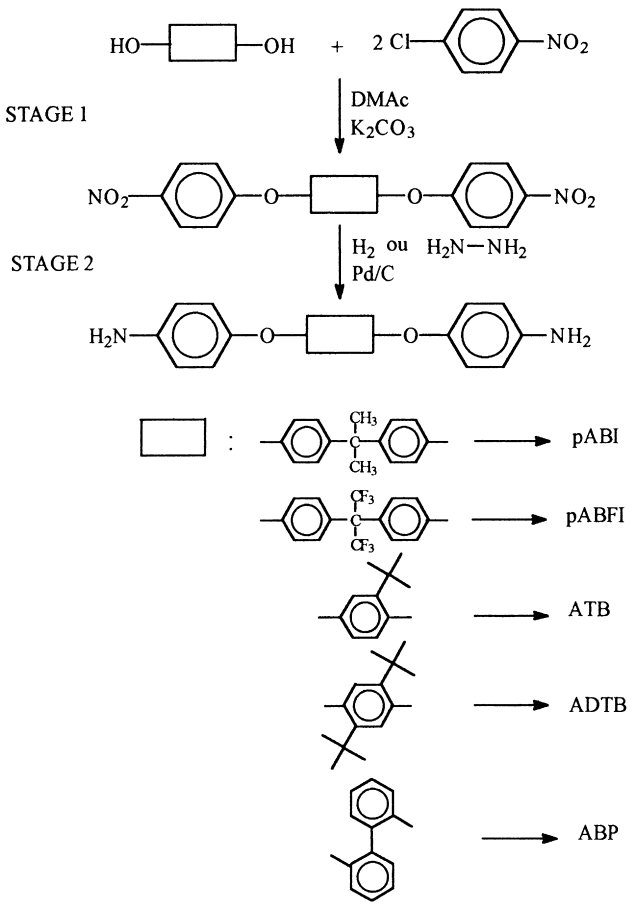


Scheme 1.

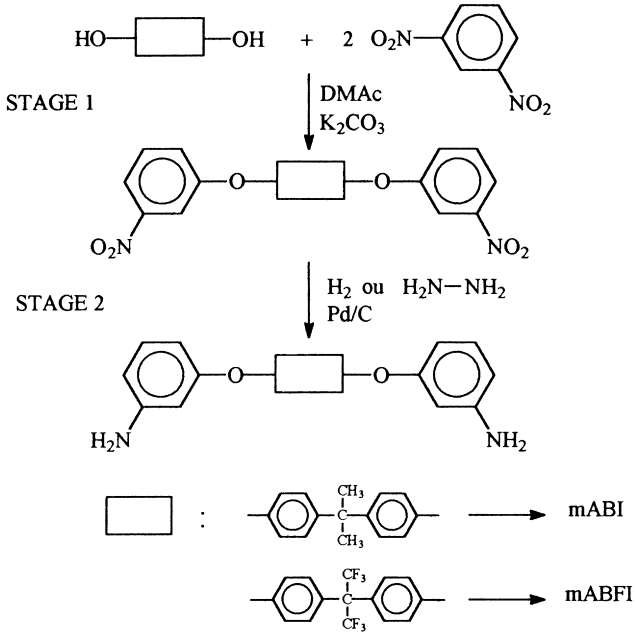


Scheme 2.

detector distance varying from 1.5 to 5 m. The samples were equilibrated in deuterated water and placed in quartz cells with a 1 mm path length. Usual corrections for the incoherent background subtraction and absolute scales normalization were applied to the data [19].

## 3. Results and discussion

### 3.1. Monomer synthesis

Para-amino-substituted diamines are synthesized from 4-chloronitrobenzene and corresponding dihydroxy compounds followed by reduction [20]. Synthesis procedure of *para*-amino-substituted ether diamine are shown in Scheme 1. *Meta*-amino-substituted diamines are synthesized from 1,3-dinitrobenzene and corresponding dihydroxy compounds by nitro-displacement reaction followed by reduction [20,21]. Synthesis procedure of *meta*-amino-substituted ether diamine are shown in Scheme 2.

### 3.2. Polyimides synthesis

The sequenced sulfonated copolyimides have been prepared by the two stage one pot method as illustrated Scheme 3. In this procedure, the dianhydride 1,4,5,8-naphthalene tetracarboxylic dianhydride (NTDA) and the diamines are polymerized in *m*-cresol at 180°C, using benzoic acid as catalyst [22–26]. Under these conditions, chain growth and imidization essentially occur spontaneously. A diamine endcapped sulfonated oligomer is first obtained by the condensation of the dianhydride NTDA and the sulfonated 2,2′-diamino-4,4′-biphenyl disulfonic acide (BDSA). The chain length of this sulfonated oligomer could be modify by varying the molar ratio of starting diamines (NTDA and BDSA). The BDSA mole number is noted *X*. In the second stage, the polycondensation reaction is gone on by adding a non-sulfonated diamine and the mole number of NTDA. Knowing non-sulfonated diamine number is *Y*, the ion-exchange capacity (IEC) of the final sulfonated block copolyimide is adjusted by the molar ratio (*X*/*Y*) of two diamines.

Based on this synthesis, using different non-sulfonated diamines, polymers with $x = 5$ and $X/Y = 30/70$ were synthesized. On the other hand, sequenced polyimides were prepared by varying IEC between 0.56 and 1.73 meq $g^{-1}$ with constant sulfonated chain length ($x = 5$) (See Table 1). Other polyimides were synthesized presenting different sulfonated chain length ($x = 3, 5$ and 9) with a constant IEC equals to 0.86 meq $g^{-1}$ from the diamines called mAPI, mAPFI and ATB (See Table 2). Some statistical polyimides were also prepared with different IEC (See Table 3). Moreover, the more IEC increases the more solubility in *m*-cresol decreases. The BDSA/NTDA/ATTB with weaker IEC was not soluble in *m*-cresol.

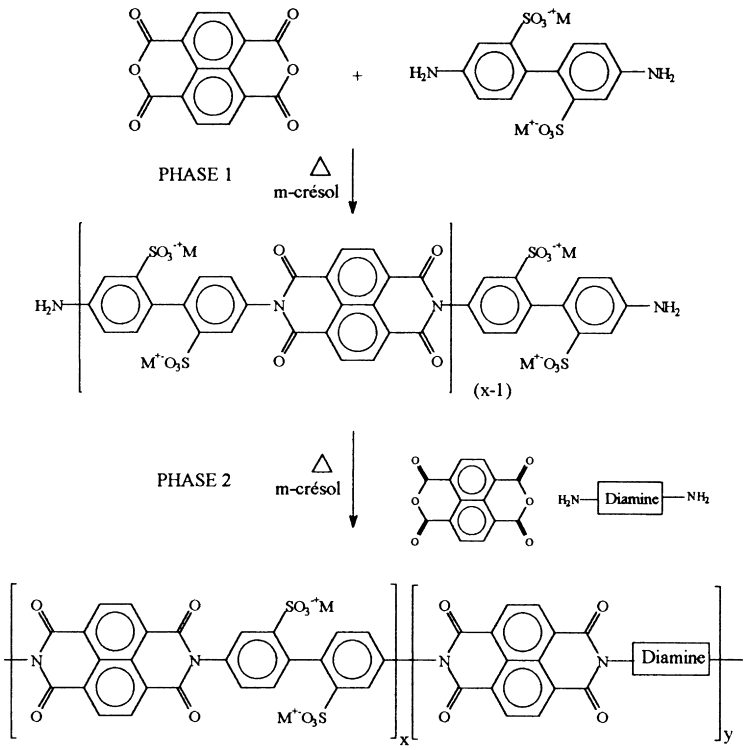


Scheme 3.

### 3.3. Polymer characterization

The chemical structure of sulfonated polyimides was confirmed by both proton and carbon NMR spectroscopy and by FTIR spectroscopy. For example, the $^1$H NMR spectrum of statistical polyimide BDSA/NTDA/ATB in triethylammonium sulfonate form is presented Fig. 2. The IR spectra (See Fig. 3) shown characteristic naphthalenic imide absorptions at near 1718 cm$^{-1}$ ($\nu_{sym}$C=O), 1680 cm$^{-1}$ ($\nu_{asym}$C=O) and 1345 cm$^{-1}$ ($\nu_{CN}$ imide). Sulfonic group absorption $\nu$(S=O) bond was observed at 1175 cm$^{-1}$. Although, we were not able to determine the molecular weight of these polymers, neither by GPC nor by light scattering, due to polymer chain associations in solution. The fact to obtain highly fibrous materials and tough films by solution casting allows us to consider these sulfonated polyimides as high molecular weight polymers.

### 3.4. Solubility study

The synthesis in *m*-cresol of some sulfonated copolyimides were not possible depending on the non-sulfonated diamine structure such as diamines called pAPI, pAPFI, ABP and ADTB and the IEC. The solubility behavior of the copolyimides in triethylammonium sulfonate form, synthesized in *m*-cresol, were studied qualitatively in some usual solvents. The results are shown in Table 4. The polymer concentration is 10%w/w. The solubility of polyimides was greatly improved by the introduction of phenylether bonds and bulky groups into the polymer backbone. Indeed, from our results, it can be seen that the solubility of polyimides from *meta*-amino-subtituted diamines (BDSA/NTDA/mAPI or mAPFI) are better than those from *para*-amino-substituted (BDSA/NTDA/ATB). However, despite the introduction of hexafluoropropylidene group in place of isopropylidene group, the solubility of corresponding polymers is approximately the same. Solubility study revealed also that statistic polyimides exhibit better solubility than sequenced polyimides in the organic solvents. It is worth noting that the homopolymers synthesized using NTDA and a non-sulfonated diamines were insoluble in *m*-cresol. The overall results indicate clearly that solubility of sulfonated polyimides seems to be governed by the hydrophobic sequence which suggests a significant effect on both the microstructure and the properties of the solution cast membranes.

### 3.5. Inherent viscosity

Inherent viscosity values, $\eta$, of sulfonated polyimides in triethylammonium sulfonate from were measured from polymer solution concentration of 0.5 g dl$^{-1}$ in *m*-cresol at 30°C. Beforehand, polymer solutions were ultrasonicated overnight to avoid large aggregate formation. These polymers are composed of a very rigid ionic sequences spaced by flexible hydrophobic sequences. As illustrated by Fig. 4a, the $\eta$(values increased with increasing IEC, the resulting apparent polymer structure is thus more and more rigid

Table 1
Structure and characteristics of polymers synthesized (ion-exchange capacity variation)

| Acronyms | *x* | *y* | IEC (meq $g^{-1}$) |
|---|---|---|---|
| BDSA/NTDA/mAPI | | | |
| 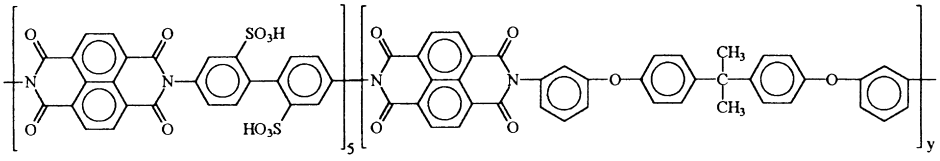 | | | |
| $CH_3$ 5 20/80 | 5 | 20.0 | 0.63 |
| $CH_3$ 5 30/70 | 5 | 11.6 | 0.96 |
| $CH_3$ 5 40/60 | 5 | 7.5 | 1.30 |
| $CH_3$ 5 50/50 | 5 | 5.0 | 1.64 |
| BDSA/NTDA/mAPFI | | | |
| 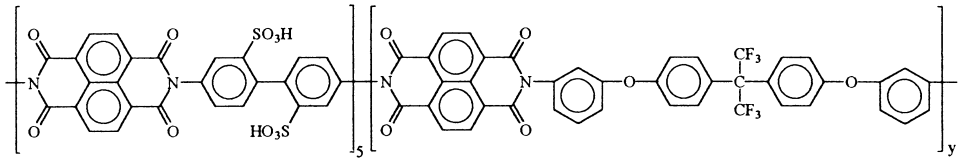 | | | |
| $CF_3$ 5 20/80 | 5 | 20.0 | 0.56 |
| $CF_3$ 5 30/70 | 5 | 11.6 | 0.86 |
| $CF_3$ 5 40/60 | 5 | 7.5 | 1.17 |
| $CF_3$ 5 50/50 | 5 | 5.0 | 1.51 |
| $CF_3$ 5 60/40 | 5 | 3.3 | 1.86 |
| BDSA/NTDA/ATB | | | |
| 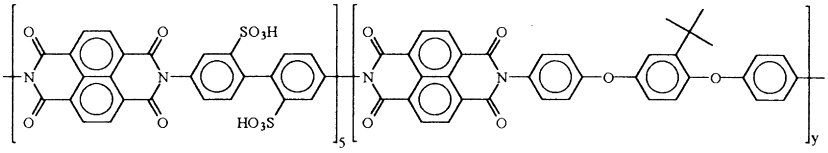 | | | |
| *t*Bu 5 30/70 | 5 | 11.6 | 1.03 |
| *t*Bu 5 40/60 | 5 | 7.5 | 1.38 |
| *t*Bu 5 50/50 | 5 | 5.0 | 1.73 |

and the overall radius of gyration increases. Fig. 4b illustrates the influence of the ionic block length on the $\eta$ values. The polymer inherent viscosity exhibit a maximum value as block lengths increases. The existence of two competitive processes can be proposed to explain the origin of this maximum. First, the polymer viscosity increases because of the increase of the polymer rigidity by increasing the rigid ionic block length. The following decrease in viscosity for ionic block length longer than four units is probably due to the low solubility in *m*-cresol of long hydrophobic sequence which could induce some polymer aggregation. We recall here that the hydrophobic homopolymer is not soluble in *m*-cresol. However, an effect due to a polymer molecular weight variation cannot be excluded since all our attempts to measure $M_w$ by gel permeation chromatography were not successful.

The inherent viscosity was then determined depending on the polymer concentration. No polyelectrolyte effect was observed in *m*-cresol on diluted polymer solution and triethylammonium neutralized form (Fig. 5). This is mainly due to the low dielectric constant of the solvent and the use of large hydrophobic counterions, which masked the ionic character of the polymer, avoiding the effect of electrostatic interactions. It is worth noting that the observed behavior

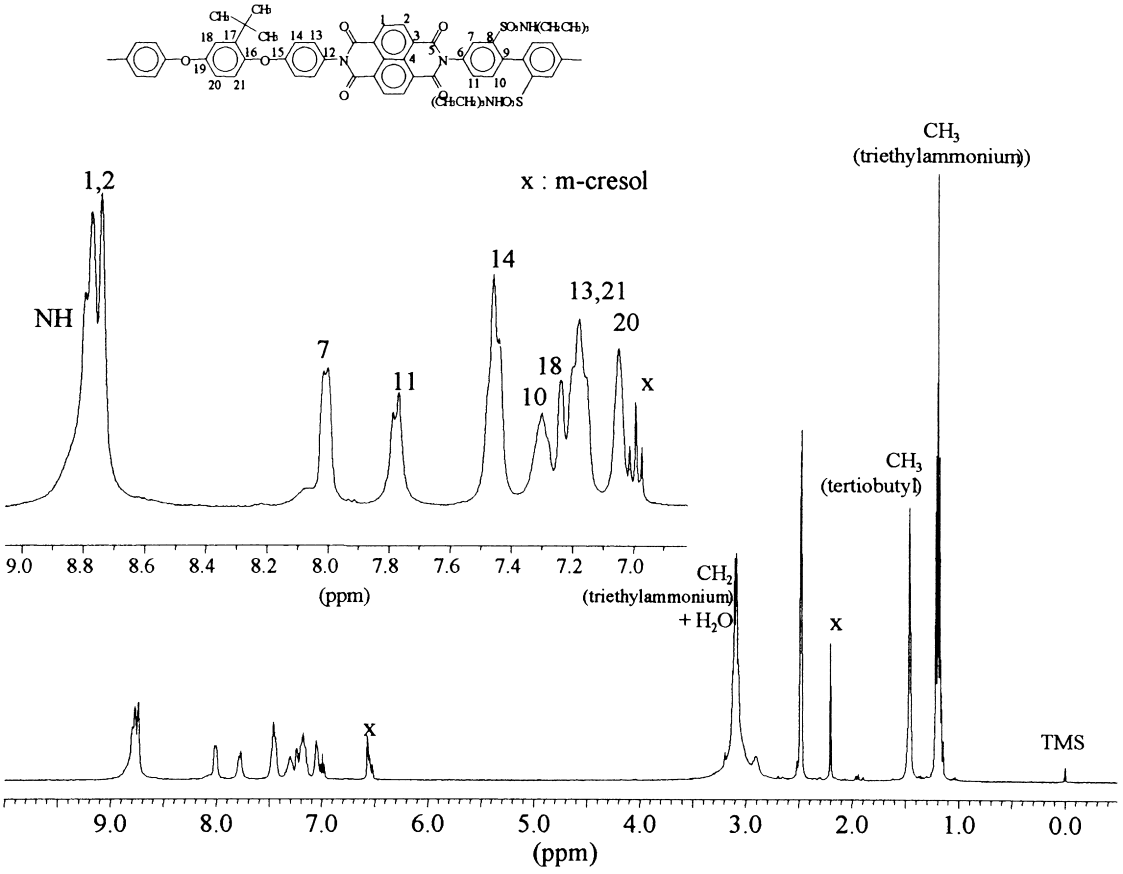


Fig. 2. $^{1}$H NMR spectrum of statistical polymer BDSA/NTDA/ATB ($X/Y = 50/50$).

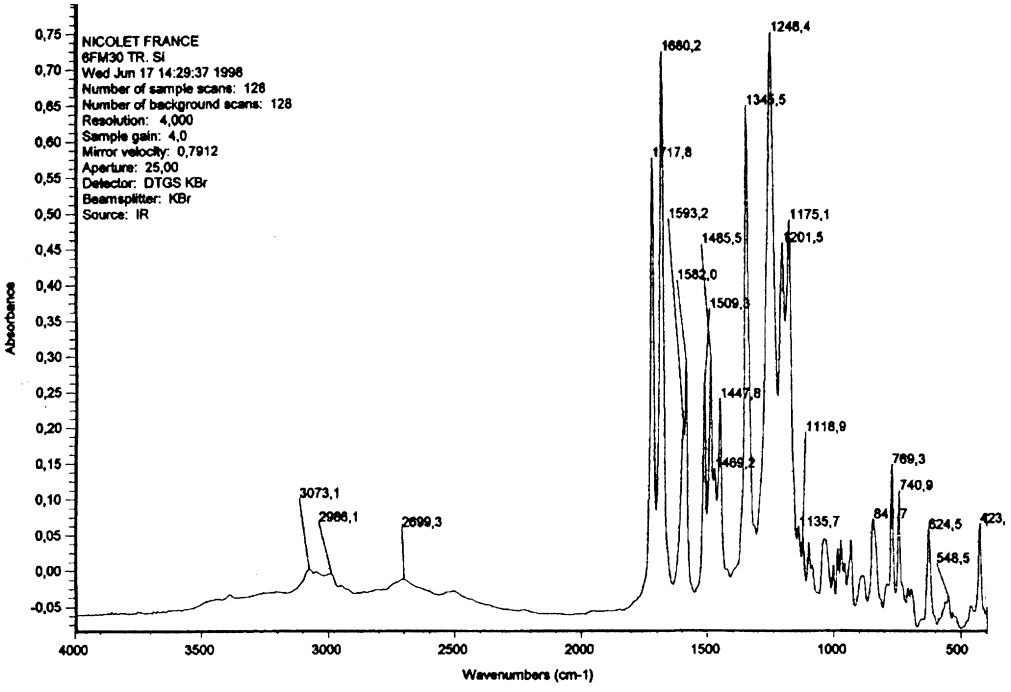


Fig. 3. IR spectrum of sequenced polymer BDSA/NTDA/mAPFI ($x = 5$ and $X/Y = 30/70$).

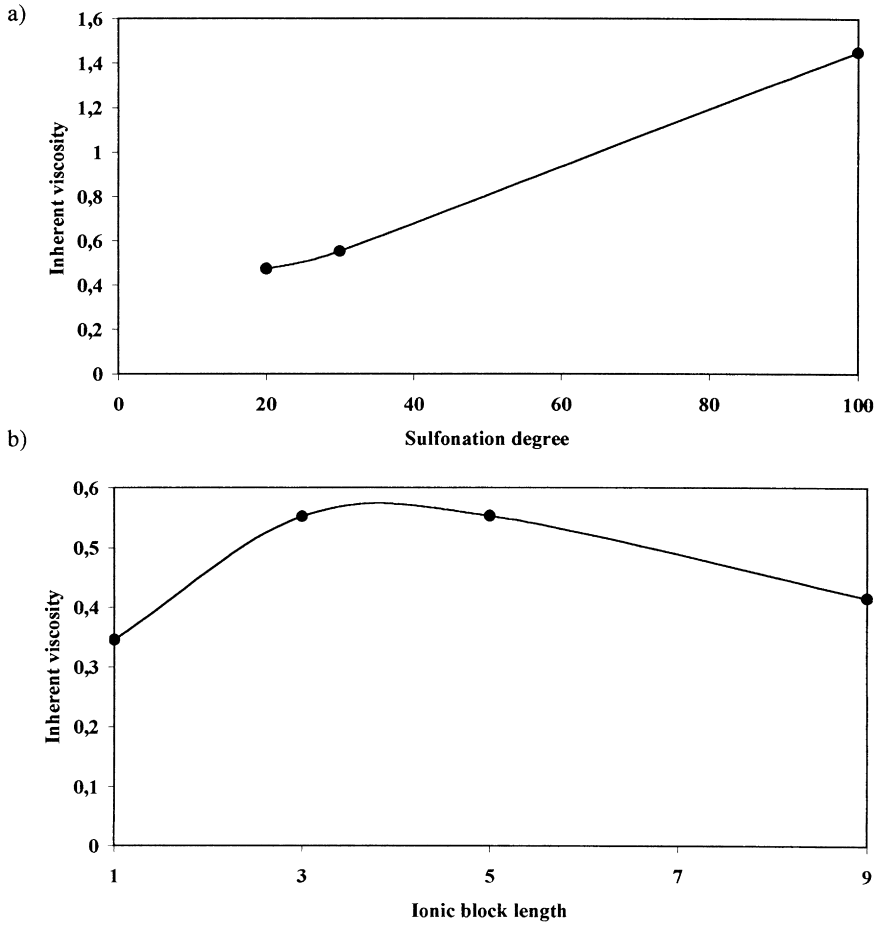


Fig. 4. Inherent viscosity data of SPI BDSA/NTSA/mAPFI solution (concentration of 0.5 g $dl^{-1}$) in *m*-cresol at 30°C against: (a) sulfonation degree; and (b) ionic block length.

which is almost linear is closer to the uncharged polymer than those giving ionomer solutions in low-polarity or non-polar solvents [27]. This result could be also attributed to the size of the triethylammonium counterion which does not favor the polymer aggregation.

### *3.6. Thermogravimetric analysis*

The thermogravimetric curves (TG) of BDSA/NTDA/mAPI sequenced polyimide ($x = 5$) with variable IEC value and different counterion are represented in Fig. 6a

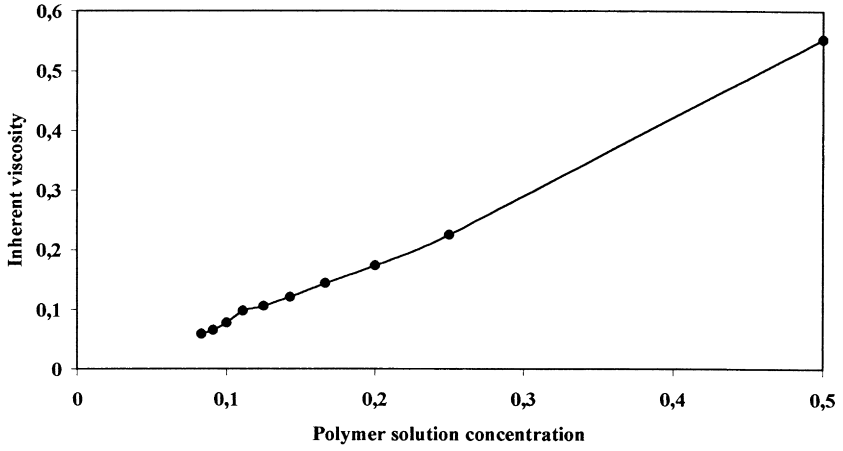


Fig. 5. Inherent viscosity data against concentration for SPI BDSA/NTDA/mAPFI solution in *m*-cresol at 30°C.

Table 2
Structure and characteristics of polymers synthesized (block length modification)

| Acronyms | x | y | IEC (meq $g^{-1}$) |
|---|---|---|---|
| BDSA/NTDA/mAPFI | | | |
| $CF_3$ 9 30/70 | 9 | 21.0 | 0.86 |
| $CF_3$ 5 30/70 | 5 | 11.6 | 0.86 |
| $CF_3$ 3 30/70 | 5 | 7.0 | 0.86 |

Table 3
Structure and characteristics of polymers synthesized (statistical polymers)

| Acronyms | x | y | IEC (meq $g^{-1}$) |
|---|---|---|---|
| $CH_3$ 1 30/70 | – | 0.96 | 0.96 |
| $CH_3$ 1 50/50 | – | 1.64 | 1.64 |
| $CF_3$ 1 30/70 | – | 0.86 | 0.86 |
| $CF_3$ 1 50/50 | – | 1.51 | 1.51 |
| *t*Bu 1 50/50 | – | 1.73 | 1.73 |

and b, respectively. The derivatives of the TG curves (DTG) are also presented so as to observe more easily the successive weight losses and their relative intensities. These curves are representative of the general thermal behavior observed for all the sequenced and statistical SPIs. The first weight loss, between 25 and 100°C, corresponds to absorbed water elimination. The second weight loss corresponds to the elimination of the residual *m*-cresol solvent. For temperatures higher than 200°C, desulfonation occurs until 400°C. The weight loss observed for a temperature higher than 420°C corresponds to the polymer backbone degradation. After proper membrane drying and MeOH washing procedures, all the polymers exhibit a thermal stability up to 200°C in both inert and oxygen atmospheres. No obvious difference in thermal stability was observed depending on the block character and between the acid and sulfonate form of SPIs ($X/Y = 40/50$) when neutralized with an ammonium counterion except the weight loss associated with the ammonium counterion (Fig. 6b).

### 3.7. Ion-exchange capacity measurements

Three different experimental methods were used to determine the ion-exchange capacity. The degree of sulfonation was first measured quantitatively by the usual titration method. Measurements were carried out for the series of BDSA/NTDA/mAPFI sulfonated polyimides. Results are recapitulated in Table 5. The degree of sulfonation was

Table 4
Solubility of sulfonated polyimides ((+ +) Soluble at room temperature, (+) soluble on heating, (−) insoluble, * gel formation after cooling, (±): partially soluble on heating)

| Acronyms | IEC (meq $g^{-1}$) | NMP | γ-Butyrolactone | Diglyme | Propylene carbonate |
|---|---|---|---|---|---|
| $CH_3$ 5 20/80 | 0.63 | + | ++ * | − | − |
| $CH_3$ 5 30/70 | 0.96 | + | ++ * | − | − |
| $CH_3$ 5 40/60 | 1.30 | + | ++ | − | − |
| $CH_3$ 5 50/50 | 1.64 | ++ | ++ | − | − |
| $CH_3$ 1 50/50 | 1.64 | + | + | − | ± * |
| $CF_3$ 5 20/80 | 0.56 | + * | ++ | − | ± * |
| $CF_3$ 5 30/70 | 0.86 | + * | ++ | − | ± * |
| $CF_3$ 5 40/60 | 1.17 | + | ++ | − | ± * |
| $CF_3$ 5 50/50 | 1.51 | + | ++ | − | ++ |
| $CF_3$ 5 60/40 | 1.86 | + | ++ | − | ++ |
| $CF_3$ 1 50/50 | 1.51 | + | + | − | + |
| *t*Bu 5 30/70 | 1.03 | ± | − | − | − |
| *t*Bu 5 40/60 | 1.38 | ± | − | − | − |
| *t*Bu 5 50/50 | 1.73 | ± | − | − | − |
| *t*Bu 1 50/50 | 1.73 | + | + | − | ± |

Table 5
Theoretical and experimental (titration method) IEC values of BDSA/NTDA/mAPFI

| Acronyms | Theoretical IEC (meq $g^{-1}$) | Experimental IEC (meq $g^{-1}$) |
|---|---|---|
| $CF_3$ 5 20/80 | 0.56 | 0.59 |
| $CF_3$ 5 30/70 | 0.86 | 0.83 |
| $CF_3$ 5 40/60 | 1.17 | 1.11 |
| $CF_3$ 5 50/50 | 1.51 | 1.42 |
| $CF_3$ 5 60/40 | 1.86 | 1.84 |
| $CF_3$ 1 50/50 | 1.51 | 1.49 |
| $CF_3$ 1 30/70 | 0.86 | 0.78 |
| $CF_3$ 1 50/50 | 1.51 | 1.49 |
| $CF_3$ 9 30/70 | 0.86 | 0.82 |
| $CF_3$ 3 30/70 | 0.86 | 0.75 |

also evaluated by the mass loss measurement by thermogravimetric analysis. The experimental values were comparable to theoretical ones. For example, the TG curves of polymer $CF_3$ 5 50/50 in acid form showed a mass loss of 12.16% and the theoretical value was 13.12%. Finally, the spectroscopy NMR was used to confirm the IEC. For instance from proton NMR polymer called tBu 1 50/50, the comparison of integral value of $CH_3$ protons corresponding to tetraethylammonium of the sulfonic groups grafted on BDSA monomer with the integral of tertiobutyl groups allows to get the *X*/*Y* value. These whole results confirm that experimental IEC values fit well the theoretical values which suggests that polymer synthesis conditions are convenient to the expected polymers.

### 3.8. Swelling and conductivity measurements

A series of information can be deduced from water uptake and conductivity measurements. Water uptake, $\lambda$ values and conductivity data determined at room temperature for polymers related to ionic-exchange capacities are recapitulated in Table 6. The water uptakes observed at 25°C for three series of sulfonated polyimides varied from 14 and 46.5% for IEC values varying from 0.5 to 1.9 meq $g^{-1}$. In a first approximation, the water uptake does not seem to depend on the nature of the non-sulfonated diamine but only on the IEC value. These water uptakes can not be easily compared each other due to the difference of density between the different polymer series. Therefore, water uptake has been expressed as the number of water molecules per ionic group ($\lambda$) defined as:

$$\lambda = \frac{n(H_2O)}{n(SO_3^-)} = \frac{WS}{18IEC}$$

where $n(H_2O)$ is the $H_2O$ mole number, ($nSO_3^-$) the $SO_3^-$ group mole number, WS the water uptake value by weight, IEC the ion-exchange capacity (eq $g^{-1}$) and 18 corresponds to water molecular weight (18 g $mol^{-1}$).

For a given polymer structure water uptake increases as ionic content increases however $\lambda$ remains constant which suggests that water is mainly located in the hydrophilic domains. In typical ionomer membranes like perfluorosulfonated or radiation-grafted membranes, the $\lambda$ value increases significantly as IEC increased and for critical IEC, the $\lambda$ value diverges due to the membrane dissolution. In the case of SPIs, the fact that $\lambda$ values are constant is surprising and could be explained by a specific morphology of membranes related to their preparation. Indeed the solvent used for solution casting and also the evaporation temperature which remains lower than the $T_g$ of these polymers are important parameters for the polymer morphology. The comparison of the $\lambda$ values between the different polymers does not indicate significant differences. Moreover, these values are also very close to those previously obtained for phthalic and naphthalenic SPIs (respectively, 12.5 and 13.2) [18]. In Table 6, it is also shown that the variation of ionic conductivity is rather weak despite the large IEC. Moreover, for the higher IEC values, the conductivity values are rather low compared to typical proton exchange membranes [28]. This is probably due to the fact that the $\lambda$ values are constant whatever the IEC. As mentioned before, the swelling remains moderate even for polymers with a high IEC. For example the ionic conductivity of BDSA/NTDA/mAPI and mAPFI reach a threshold of IEC higher

Table 6
Water uptake and conductivity values of sulfonated polyimides (ion-exchange capacity variation)

| Acronyms | IEC (meq $g^{-1}$) | Water uptake (%w/w) | $\lambda$ ($H_2O$ molecules/$SO_3^-$) | $\sigma \times 10^{-3}$ (S $cm^{-1}$) |
|---|---|---|---|---|
| $CH_3$ 5 20/80 | 0.63 | 13.5 | 12.5 | 0.32 |
| $CH_3$ 5 30/70 | 0.96 | 19.0 | 11.5 | 1.3 |
| $CH_3$ 5 40/60 | 1.30 | 27.0 | 12.0 | 6.5 |
| $CH_3$ 5 50/50 | 1.64 | 42.0 | 15.0 | 5.9 |
| $CF_3$ 5 20/80 | 0.56 | 14.0 | 14.0 | 0.40 |
| $CF_3$ 5 30/70 | 0.86 | 22.0 | 14.0 | 1.7 |
| $CF_3$ 5 40/60 | 1.17 | 31.0 | 15.0 | 4.6 |
| $CF_3$ 5 50/50 | 1.51 | 41.0 | 15.0 | 7.1 |
| $CF_3$ 5 60/40 | 1.86 | 46.5 | 14.0 | 8.3 |
| *t*Bu 5 30/70 | 1.03 | 24.5 | 13.0 | 0.04 |
| *t*Bu 5 40/60 | 1.38 | 45.5 | 18.0 | 3.1 |
| *t*Bu 5 50/50 | 1.73 | 45.5 | 15.0 | 6.7 |

Table 7
Water uptake and conductivity values of sulfonated polyimides (block length modification)

| Acronyms | IEC (meq $g^{-1}$) | Water uptake (%) | $\lambda$ ($H_2O$ molecules/$SO_3^-$) | $\sigma \times 10^{-3}$ (S $cm^{-1}$) |
|---|---|---|---|---|
| $CF_3$ 1 30/70 | 0.86 | 19.5 | 12.5 | 1.1 |
| $CF_3$ 3 30/70 | 0.86 | 17.0 | 11.0 | 2.7 |
| $CF_3$ 5 30/70 | 0.86 | 22.0 | 14.0 | 1.7 |
| $CF_3$ 9 30/70 | 0.86 | 20.0 | 13.0 | 0.36 |

than 1.3 meq $g^{-1}$. This observation confirms that there is a relation between the water swelling and the conductivity through the concept of ionic domain percolation. For low IEC values, the conductivity is limited by the connection between ionic domains. By increasing IEC, the ionic domains are more and more inter-connected and, above the percolation threshold, the level of interconnection is large enough to be not more the limiting parameter for the diffusion process. Therefore, the ionic conductivity increases up to a maximum value because the ion concentration is constant in the ionic domains (constant $\lambda$ values) and the ion mobility in the ionic domains is expected to be identical for all samples. The only important parameter is thus the ionic phase volume fraction which variation with IEC is small for large values.

Water uptake and conductivity values for polymers according to ionic sequence length are given in Table 7. The ionic conductivity exhibits a maximum value for a ionic block average length equal to 3 monomer units. It is worth noting that the conductivity variation is rather large (almost a factor 10) and does not follow the evolution of the water uptake which is almost

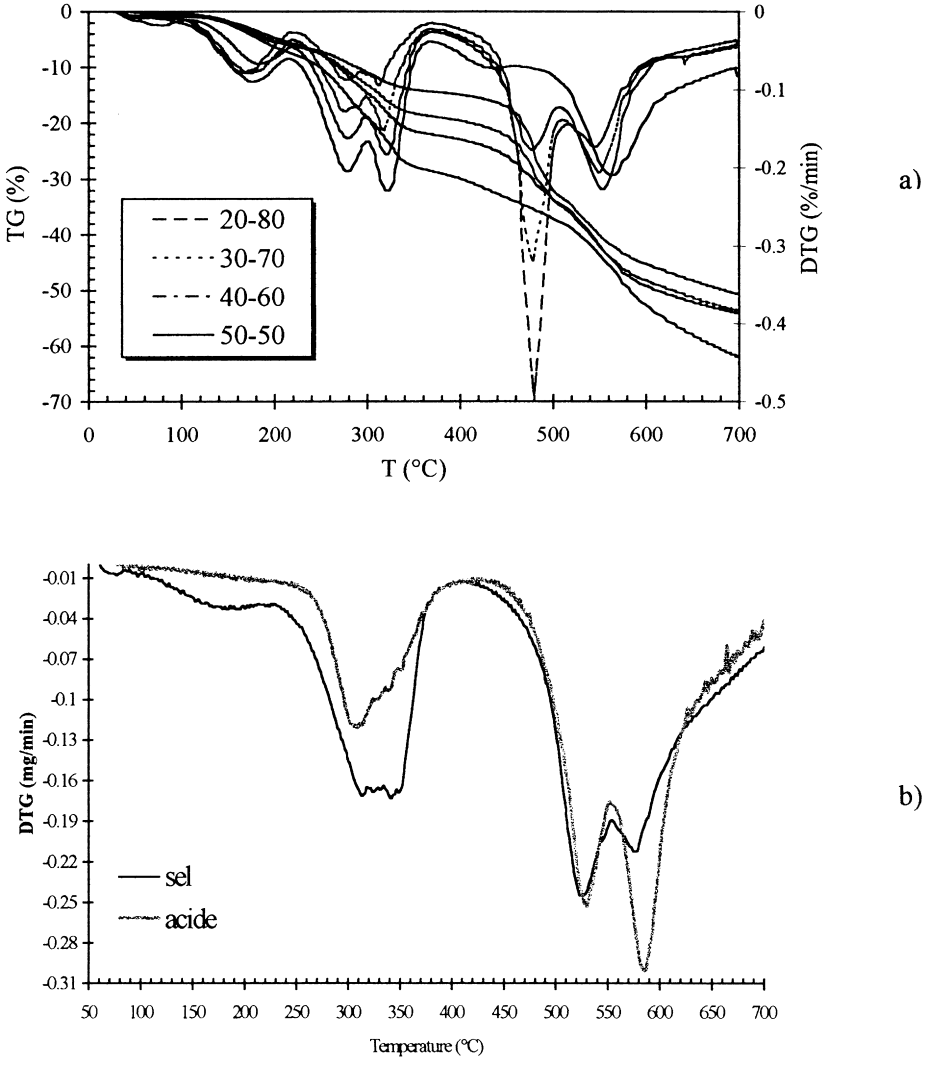


Fig. 6. Thermogravimetric curves for BDSA/NTDA/mAPI sequenced ($x = 5$) SPIs: (a) effect of IEC; (b) acidic versus triethylammonium forms.

Table 8
Water uptake and conductivity values of sulfonated polyimides (statistic polymers)

| Acronyms | IEC (meq $g^{-1}$) | Water uptake (%) | $\lambda$ ($H_2O$ molecules/$SO_3^-$) | $\sigma \times 10^{-3}$ (S $cm^{-1}$) |
|---|---|---|---|---|
| $CH_3$ 1 30/70 | 0.96 | 11.0 | 7.0 | 0.91 |
| $CH_3$ 5 30/70 | 0.96 | 19.0 | 11.5 | 1.3 |
| $CH_3$ 1 50/50 | 1.64 | 31.0 | 11.0 | 4.6 |
| $CH_3$ 5 50/50 | 1.64 | 42.0 | 15.0 | 5.9 |
| $CF_3$ 1 30/70 | 0.86 | 19.5 | 12.5 | 1.1 |
| $CF_3$ 5 30/70 | 0.86 | 22.0 | 14.0 | 1.7 |
| $CF_3$ 1 50/50 | 1.51 | 25.0 | 9.5 | 6.1 |
| $CF_3$ 5 50/50 | 1.51 | 41.0 | 15.0 | 7.1 |
| *t*Bu 1 50/50 | 1.73 | 40.5 | 13.0 | 5.1 |
| *t*Bu 5 50/50 | 1.73 | 45.5 | 15.0 | 6.7 |

constant. The maximum value of the conductivity is even obtained for the sample presenting the lower water uptake. This result is not in agreement with the general rule which says that the ionic conductivity of ion-exchange membranes is strongly related to the water content of the membrane. A possible explanation of the existence of a maximum value depending of the ionic sequence length is that the sequenced character favors the phase separation and consequently the conductivity. However, for long sequences, the length of the inter-domain connections increases which induce a decrease of the conductivity. The fact that the same evolution is observed for both the solution inherent viscosity and the bulk membrane conductivity versus the block length was considered as a coincidence.

In Table 8, the water uptake and conductivity values are compared for sequenced and statistical polyimides having the same IEC. Both $\lambda$ and conductivity values are systematically lower for statistical compared to block copolyimides. The observation is in good accordance with an ionic phase separation of the block copolymers. However, the difference in conductivity between sequenced and statistical polymers decreases when IEC increases (See Table 8). In this case, the high sulfonic acid group concentration allows the proton conduction across the membrane whatever the ion distribution along the polymer chain.

### 3.9. Small-angle neutron scattering

Preliminary SANS experiments were carried out over an extended angular range on both statistical and sequenced polymers ($CH_3$ 5 30/70) (Fig. 7). A broad scattering maximum characteristic of bulk ionic polymers (so-called "ionomer peak") due to the phase separation between ionic domains and the hydrophobic polymer matrix was observed. Previous SANS experiments performed with flexible phthalic and very rigid naphthalenic sulfonated polyimides revealed the existence of very large ionic domains attributed to the block character of the polymers [18]. The important result of this previous work was the presence of a well defined ionomer peak with the flexible polymer while no ionomer peak was observed for the rigid polymer despite a high level of the scattered intensity. In the present work, the sequenced polymer also exhibits a well defined ionomer peak. The second important result is the fact that the position of the ionomer peak is located at an angle roughly five times lower for the sequenced polymer compared to the statistical polymer. Since the ionic sequenced is five times longer for the sequenced polymer, it can be concluded that the peak corresponds to an interference peak between ionic domains and that their dimension is roughly proportional to the ionic sequence length.

### 3.10. Hydrolysis stability

The polymer BDSA/NTDA/mAPI and mAPFI 5 30/70 in acid form exhibited an hydrolysis stability during around 200 h in distilled water at 80°C characterized by the loss of the mechanical properties, namely the membrane becomes highly brittle. This result is intermediary between the hydrolysis behavior of phthalic copolyimide BDSA/ODPA/ODA (the acronym ODPA correspond to oxydiphthalic dianhydride) which was stable only during few minutes and the naphthalic copolyimide BDSA/NTDA/ODA one which was stable around 1000 h in the same

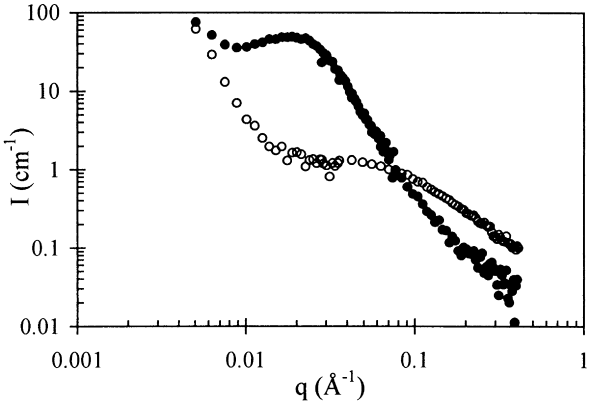


Fig. 7. SANS spectra obtained for swollen statistical (○) and $x = 5$, $X/Y = 40/60$ sequenced (●) SPI copolymers (BDSA/NTDA/mAPFI).

conditions. It is worth noting that the membrane thickness was not the same for all the polymers. The thickness of membranes BDSA/NTDA/mAPI and mAPFI was around 20 μm whereas the one of others membranes is around 100 μm). The influence of the membrane thickness on the hydrolysis stability is at the present time under consideration.

## 4. Conclusion

Aromatic ether diamines having different amino-substituted positions and/or bulky groups in their structure were synthesized. Using three of these synthesized ether diamines, naphthalenic tetracarboxylic dianhydride and sulfonated diamine, new soluble sequenced and statistic sulfonated polyimides having different IEC with varying block lengths were prepared by copolycondensation. The sulfonated polyimide structure was confirmed by NMR, IR spectroscopy. Ionic character of these polymers allows to obtain water uptake varying from 13 to 45% for IEC between 0.5 and 1.9 meq $g^{-1}$. The main result is that the $\lambda$ value is roughly constant over the IEC range. The ionic conductivity values are in the order of few mS $cm^{-1}$ at room temperature which values remain quite weak compound to 0.1 S $cm^{-1}$ required for fuel cell application. A preliminary SANS study indicates the existence of large ionic domains which size seems to be proportional to the ionic block length. The determination of structure–properties relationship will the subject of a forthcoming paper.

## Acknowledgements

The authors would like to thank J. Teixeira as local contact and the LLB laboratory for their help in realizing SANS experiments. One of us (C.G.) is indebted to the CEA of Grenoble and specially the DRFMC/SI3M/PCI laboratory for financial support.

## References

[1] Risen WM. In: Schlick S, editor. Ionomers: characterization, theory, and applications, Boca Raton, FL: CRC Press, 1996.
[2] Boucher-Sharma AP, Chowdhury G, Matsuura T. J Appl Polym Sci 1997;74:47.
[3] Chowdhury G, Matsuura T, Sourirajan S. J Appl Polym Sci 1994;51:1071.
[4] Fu H, Jia L, Xu J. J Appl Polym Sci 1994;51:1399.
[5] Fu H, Jia L, Xu J. J Appl Polym Sci 1994;51:1405.
[6] Noshay A, Robeson LM. J Appl Polym Sci 1976;20:1885.
[7] Tan L-S, Arnold FE, Chuah HH. Polymer 1991;32:1376.
[8] Sarkar N, Kershner LD. J Appl Polym Sci 1996;62:393.
[9] Karcha RJ, Porter RS. Polymer 1992;33:4866.
[10] Lu X, Weiss RA. Macromolecules 1992;25:6185.
[11] Samuelson LA, Anagnostopoulos A, Alva KS, Kumar J, Tripathy SK. Macromolecules 1998;31:4376.
[12] Pak YS, Xu G. Solid State Ionics 1993;67:165.
[13] Yeager AL, Steck A. J Electrochem Soc 1981;128:1880.
[14] Scherer GG. Ber Bunsenges Phys Chem 1990;94:1008.
[15] Savadogo O. J New Mater Electrochem Systems 1998;1:47.
[16] Wakizoe M, Velev O, Srinivasan S. Electrochim Acta 1995;40:335.
[17] Faure S, Mercier R, Aldebert P, Pineri M, Sillion B. French Pat. 96 05707, 1996.
[18] Faure S, Cornet N, Gebel G, Mercier R, Pineri M, Sillion B. Proceedings of Second International Symposium on New Materials for Fuel Cell and Modern Battery Systems, Montreal, Canada, July 6–10, 1997. p. 818.
[19] Cotton JP. In: Lindner P, Zemb T, editors. Neutron, X-rays and light scattering: introduction to an investigate tool for colloidal and polymeric systems, Amsterdam: Elsevier, 1991. p. 19.
[20] Tamai S, Yamaguchi A. Polymer 1996;37:3683.
[21] Liou G-S, Maruyama M, Kakimoto M-A, Imai Y. J Polym Sci, Part A: Polym Chem 1993;31:3273.
[22] Rusanov AL. Adv Polym Sci 1994;111:115.
[23] Sek D, Wanic A, Schab-Balcerzak E. J Polym Sci, Part A: Polym Chem 1997;35:539.
[24] Gao JP, Wang ZY. J Polym Sci, Part A: Polym Chem 1995;33:1627.
[25] Loughran GA, Arnold FE. Polym Prepr 1977;18:831.
[26] Jedlinski ZJ, Kowalski B, Gaik U. Macromolecules 1983;17:522.
[27] Hara M, Wu J-L, Lee AH. Macromolecules 1988;21:2214.
[28] Yeo R, Yeager H. Modern aspects of electrochemistry: structural and transport properties of perfluorinated ion-exchange membranes, vol. 16, 1985. p. 437.